

DD

LBL-37975
UC-406
Preprint



Lawrence Berkeley Laboratory

UNIVERSITY OF CALIFORNIA

Submitted to IEEE Transactions on Nuclear Science

Characterization of a 64 Channel PET Detector Using Photodiodes for Crystal Identification

W.W. Moses, S.E. Derenzo, M.H. Ho, M.S. Andreaco,
C.W. Williams, M.J. Paulus, and R. Nutt

November 1995



CERN LIBRARIES, GENEVA

SC9612

**Biology &
Medicine
Division**

DISCLAIMER

This document was prepared as an account of work sponsored by the United States Government. Neither the United States Government nor any agency thereof, nor The Regents of the University of California, nor any of their employees, makes any warranty, express or implied, or assumes any legal liability or responsibility for the accuracy, completeness, or usefulness of any information, apparatus, product, or process disclosed, or represents that its use would not infringe privately owned rights. Reference herein to any specific commercial product, process, or service by its trade name, trademark, manufacturer, or otherwise, does not necessarily constitute or imply its endorsement, recommendation, or favoring by the United States Government or any agency thereof, or The Regents of the University of California. The views and opinions of authors expressed herein do not necessarily state or reflect those of the United States Government or any agency thereof or The Regents of the University of California and shall not be used for advertising or product endorsement purposes.

Lawrence Berkeley Laboratory is an equal opportunity employer.

Characterization of a 64 Channel PET Detector Using Photodiodes for Crystal Identification

W.W. Moses,* S.E. Derenzo,* M.H. Ho,* M.S. Andreaco,**
C.W. Williams,** M.J. Paulus,** and R. Nutt**

*Life Sciences Division, Lawrence Berkeley Laboratory
University of California, Berkeley, CA 94720

**CTI PET Systems
Knoxville, TN

November 1995

This work was supported in part by the Director, Office of Energy Research, Office of Health and Environmental Research, Medical Applications and Biophysical Research Division, of the U.S. Department of Energy under Contract No. DE-AC03-76SF00098, and by Public Health Service Grant Nos. P01-HL25840, R01-CA48002, and R01-NS29655.

CHARACTERIZATION OF A 64 CHANNEL PET DETECTOR USING PHOTODIODES FOR CRYSTAL IDENTIFICATION*

W.W. Moses[†], S.E. Derenzo[†], M.H. Ho[†], M.S. Andreaco[‡], C.W. Williams[‡], M.J. Paulus[‡], and R. Nutt[‡],
[†]Life Science Division, Lawrence Berkeley Laboratory, Berkeley, CA, and [‡]CTI PET Systems, Knoxville, TN

Abstract

We present performance results for prototype PET detector modules consisting of 64 scintillator crystals (3x3x25 mm BGO crystals and 3x3x20 mm LSO crystals) coupled on one end to a single photomultiplier tube and on the opposite end to a 64 pixel array of 3 mm square silicon photodiodes (typically pixel parameters are 5 pF capacitance, 300 pA dark current, 73% quantum efficiency). The photomultiplier tube provides an accurate timing pulse and energy discrimination for the all the crystals in the module, while the silicon photodiodes identify the crystal of interaction. With 16 of the channels instrumented, both the BGO and LSO based detector modules correctly identify the crystal of interaction (where "correct" includes the adjacent 4 crystals) roughly 80% of the time with high detection efficiency, although the LSO based detector module achieves this correct identification fraction with higher detection efficiency than the BGO module. The timing resolution for a single LSO detector module is 750 ps fwhm, while its pulse height resolution is about 50% fwhm.

1. INTRODUCTION

We have previously presented design studies and prototype results for several high rate, high resolution PET detector modules that utilize a single photomultiplier tube to provide an accurate timing pulse and initial energy discrimination for a group of 3 mm square by 25–30 mm deep scintillator crystals and a silicon photodiode array to identify the crystal of interaction and possibly the depth of interaction (figure 1a). These studies have shown encouraging room temperature results with both BGO scintillator (which is only capable of identifying the crystal of interaction) [1] and LSO scintillator (which is also capable of measuring depth of interaction) [2].

However, the prototype detector modules used to obtain these results had a maximum of four scintillator crystal / photodiode elements due to the lack of a suitable 64 element photodiode array. This raises questions about whether the technologies employed can be scaled up to a full 64 element detector module and still yield a practical design. In this paper we report results of measurements made on 64 element detector modules made with both BGO and LSO scintillator crystal.

2. INDIVIDUAL COMPONENTS

A. Scintillator Crystal Arrays

Two detector modules were made by coupling 64 element

scintillator crystal arrays onto 1" square Hamamatsu R-2497 photomultiplier tubes. One array had 2.5 x 2.5 x 25 mm BGO scintillator crystals (shown in figure 1b) arranged into an 8x8 array on a 3 mm pitch, with the gap between crystals filled with white reflector material. The array was prepared with a roughened surface treatment and diffuse reflector material.

The other detector module used 2.7 x 2.7 x 20 mm LSO scintillator crystals, again arranged into an 8x8 array on a 3 mm pitch. Several compromises were made due to the limited availability of LSO scintillator material (grown by Schlumberger-Doll Research). The length of the crystal was 20 mm because of insufficient starting material long enough to make 25 mm long crystals. Individual crystals came from a number of separate growth runs and had lower than "typical"

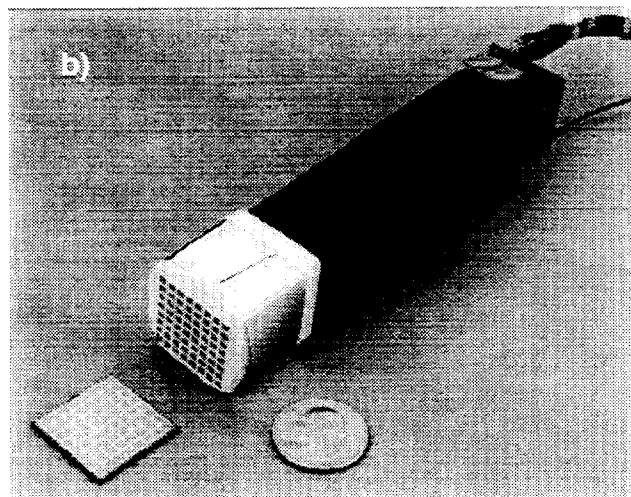
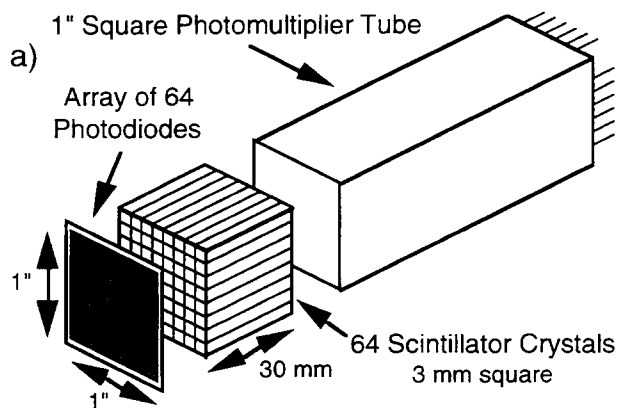


Figure 1: a) Diagram of the PET module. Each crystal is attached to a photomultiplier tube, which provides timing and initial energy information, and to a photodiode, which identifies the crystal of interaction. The PMT and PD signals can be combined to measure the depth of interaction. b) Photograph of the 64 channel BGO detector module. The PMT, BGO crystal array, and photodiode array are shown prior to attaching the photodiode array.

* This work was supported in part by the U.S. Department of Energy under Contract No. DE-AC03-76SF00098, and in part by Public Health Service Grant Nos. P01-HL25840, R01-CA48002, and R01-NS29655.

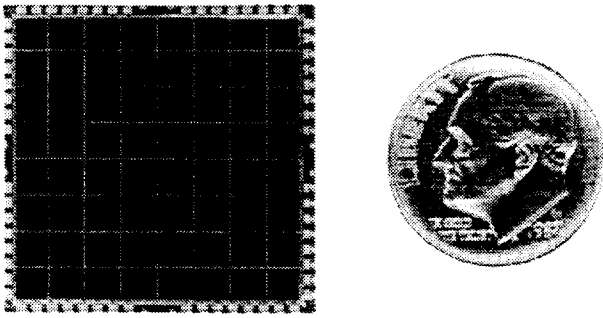


Figure 2: Photograph of the 64 element photodiode array. Each element has a 3–6 pF capacitance and a 200–400 pA dark current.

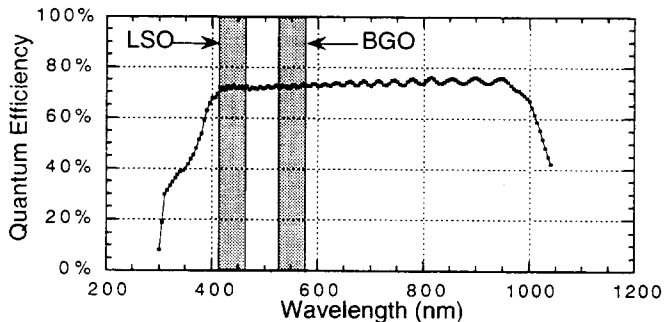


Figure 3: Quantum efficiency vs. wavelength for the photodiode array, showing 73% quantum efficiency for both BGO and LSO.

LSO light output. The mean light output was approximately 12,000 photons/MeV — higher than BGO but half of “typical” LSO and one third of the best LSO. Due to the low light output, a depth of interaction module with a “diffuse” reflector coating was not attempted, and the individual crystals were polished on all six faces and the gaps between crystals filled with white RTV reflector material. After being fabricated into an array, large crystal to crystal variations in light output were observed, and are discussed in Section 4.

B. Photodiode Array

Each pixel of the 64 element, 3 mm pitch photodiode array (provided by Hamamatsu Photonics) was 2.8 mm square, except for those elements on the periphery. Because electrical connections to the photodiode elements are made on a 1.2 mm wide optically inactive region around the perimeter of the diode array, the size of the corner elements was reduced to 2.5 mm square and the remainder of the elements on the periphery reduced to 2.5 x 2.8 mm. This degrades the optical coupling to the crystal elements on the edge of the detector array, but allows the inactive region (*i.e.* insensitive to 511 keV gamma rays) between two adjacent detector modules to be reduced from 2.4 mm to 1.8 mm. A photograph of the photodiode array is shown in figure 2.

The silicon PIN photodiode array has a 300 μm depletion thickness and each element has a 3–6 pF capacitance (measured at the perimeter of the array), with elements toward the center having higher capacitance due to the longer lead length. With a 50 V bias, the dark current at 25° C was 200–

400 pA per element, with no systematic dependence on location. The quantum efficiency, shown in figure 3, is approximately 73% both for the 480 nm emissions of BGO and the 415 nm emissions of LSO.

C. Electronics

Amplification for the photodiodes is provided by 2 mm square custom ICs containing 16 low noise charge sensitive preamplifiers and shaper amplifiers [3]. Because of a design error in this preamplifier, the noise performance when coupled to the photodiode (220 e^- RMS) is significantly worse than the design noise of 125 e^- RMS. An amplifier peaking time of 750 ns was used for all measurements.

The crystal of interaction is determined using a custom CAMAC module that amplifies and simultaneously samples 16 voltages (the outputs of one amplifier IC), then passes the 16 held analog voltages to a scanning ADC for digitization and computer readout. This configuration has relatively low rate capability (~ 1 khz), but allows low level signals to be measured and gain corrections to be applied to each element.

An alternative method for rapidly (< 50 ns) identifying the crystal of interaction is a “Winner-Take-All” (WTA) circuit that, given n analog input voltages, rapidly determines which input has the highest voltage and outputs the encoded address of this channel [4]. This approach is more desirable than a threshold discriminator approach, as it ensures that *exactly* one channel is identified on every event. This is especially important for Compton interactions with energy deposit in more than one crystal element. We have built a 16 input integrated circuit of this type that includes a common strobe sample and hold on each input (so that the channels can be simultaneously compared) and a buffered analog output that is proportional to the voltage of the “winner” (*i.e.* the channel with the highest voltage). The voltage of the “winner” can then be compared to the PMT energy signal to determine the depth of interaction.

Unfortunately, the WTA circuit was not used in these measurements. The WTA requires the “winner” to be > 30 mV higher than the second highest voltage, and due to insufficient amplifier gain and the low light output from these scintillator arrays (the intrinsic “low” luminosity of BGO and the poor quality of the LSO), the voltage corresponding to a 511 keV energy deposit was not sufficiently above this 30 mV threshold to ensure proper identification. In addition, large crystal to crystal light output variations (as large as a factor of 3) in the LSO array required channel to channel gain compensation, which is not possible in the present amplifier IC.

3. BGO DETECTOR PERFORMANCE

Since the crystal of interaction in the 64 element BGO module was identified using the CAMAC amplifier and sample / hold board, the number of instrumented channels was limited to 16. The detector module was excited with a beam of 511 keV photons that was electronically collimated (2.0 mm fwhm) using a single 3 x 3 x 30 mm BGO crystal coupled to a photomultiplier tube, and aligned with a “target” crystal in the detector module. Whenever the photomultiplier tube

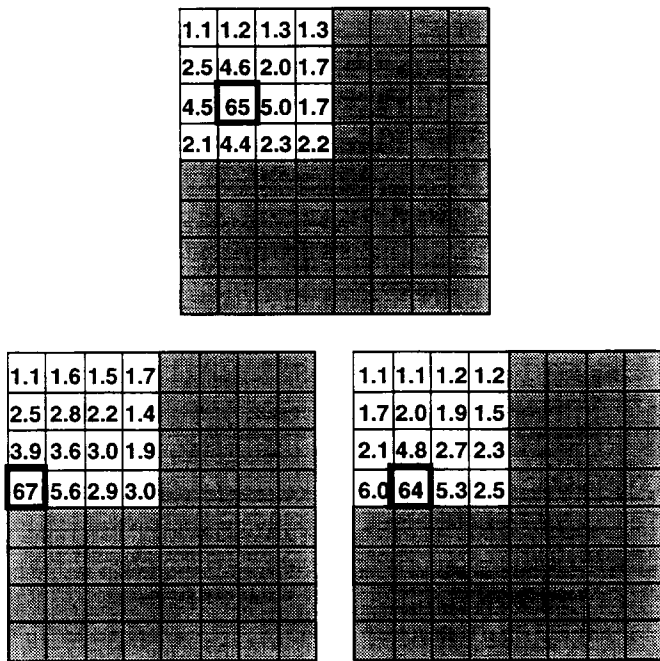


Figure 4: Using the BGO detector, the percentage of the time that each element is identified as the crystal of interaction for three “target” positions (identified by the thick border). Darkened regions indicate elements without amplifiers.

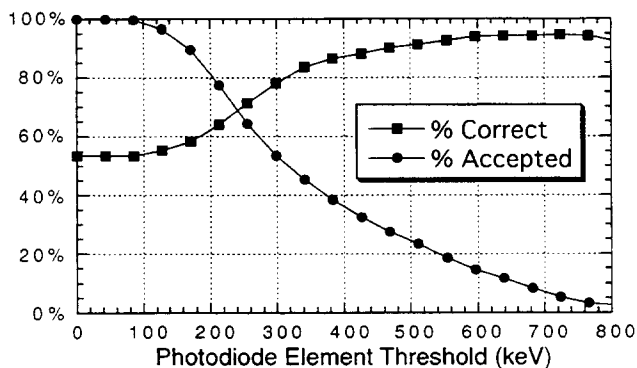


Figure 5: Percentage of events accepted and correctly identified in the BGO detector module as a function of photodiode element threshold voltage. The “target” element used is shown in the upper portion of figure 4.

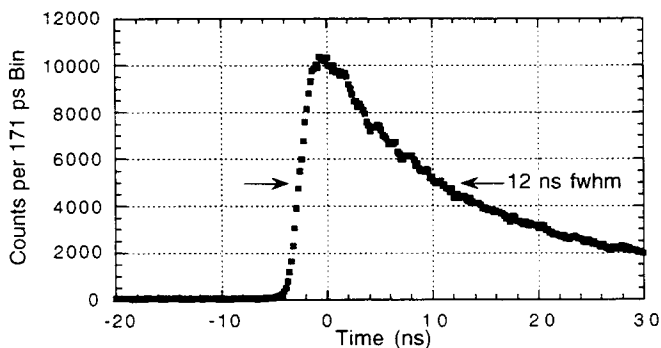


Figure 6: Coincidence timing resolution (with plastic scintillator) for the BGO detector module with a single photon threshold.

detected an energy deposit greater than 100 keV (in time coincidence with the collimating photomultiplier tube), signals from the 16 instrumented elements were read out and the channel with the greatest pulse height was then defined to be the crystal of interaction, provided that it was above a specified energy threshold.

Figure 4 shows several end-on views of the 8 by 8 array of square scintillator crystals, each with a different “target” crystal (identified by a heavy border). The numbers in each square represent the percentage of photomultiplier tube triggers in which the interaction was assigned to that crystal. Thus, figure 4 shows that for the photodiode energy threshold used (225 keV), the correct crystal of interaction is assigned approximately 65% of the time. This compares very favorably with conventional block detectors, which typically obtain 50% correct identification fraction with 4 mm square crystals [5].

There are three main effects that cause crystals other than the “target” crystal to be identified — imperfect collimation of the excitation beam, Compton scatter in the detector module, and electronic noise. Both imperfect collimation and detector Compton scatter lead to the adjacent 4 crystals being identified as the crystal of interaction more often than the other non-target crystals. It is difficult to separate these two effects, but Monte Carlo simulation suggests that Compton scatter alone results in each of the adjacent 4 crystals being identified 6% of the time [6], while imperfect collimation with a 2.0 mm fwhm beam results in each of the adjacent 4 crystals being illuminated 3% of the time. These misidentification fractions in adjacent crystals are consistent with the measured fractions.

The value of the photodiode energy threshold affects both the fraction of correctly identified events (as defined above), and the fraction of accepted events (defined as the fraction of those PMT triggers in which the maximum element is above the threshold energy). Figure 5 plots the fraction of accepted events (with a PMT trigger threshold of 100 keV) and correctly identified events as a function of the threshold energy.

It is not possible to measure the pulse height resolution in this detector, as the reflector coating had pronounced depth of interaction effects (a factor of 3 from one end of the crystal to the other). However, the signal to noise ratio in the photodiode array at room temperature is insufficient to take advantage of this effect and measure the depth of interaction on an event by event basis.

The depth of interaction dependence also affects the timing resolution, which is determined by simultaneously exciting this detector module and a reference detector (plastic scintillator coupled to a fast photomultiplier tube) with annihilation photons and measuring the time difference between the reference detector and the photomultiplier tube discriminator output (with a single photoelectron threshold). The timing distribution, shown in figure 6, has a pronounced tail toward longer times and poor (12 ns fwhm) timing resolution. This tail is caused by interactions close to the photodiode end of the detector module which, due to the reduced signal at the photomultiplier tube, have a lower photoelectron rate after excitation and so tend to produce a “late” timing signal.

4. LSO DETECTOR PERFORMANCE

Due to the unusually low light output of the LSO crystals used, the CAMAC amplifier and sample / hold board was also used to identify the crystal of interaction with the LSO module, again limiting the number of instrumented channels to 16. However, this allowed channel to channel correction for variations in the light output of the individual scintillator crystals, which were as high as 3:1 (see the pulse height spectra in figure 7). Figure 7 also shows that the 511 keV energy resolution of the detector is approximately 50% fwhm.

The LSO module was characterized using methods similar to those described in the previous section, except that the size of the collimated beam of 511 keV photons was larger (2.8 mm fwhm) due to geometrical differences in the detector module enclosures. The results shown in figure 8 (obtained with a 300 keV photodiode energy threshold) suggest that the LSO module has a lower correct crystal identification than the BGO module. However, we believe this to be an artifact of the poorer beam collimation. A 2.8 mm fwhm beam centered on a 3 mm square "target" crystal only illuminates that crystal 65% of the time, with each of the adjacent 4 crystals being illuminated 8% of the time. This is significantly worse than the 85% illumination of the "target" crystal (and 3% illumination on each of the 4 adjacent crystals) with a 2.0 mm fwhm beam.

Figure 9 plots the fraction of accepted events and correctly identified events as a function of the photodiode threshold energy. The effect of imperfect beam collimation can be somewhat reduced by redefining "correct" to be either the "target" crystal or one of the 4 adjacent crystals. With this definition, the crystal of interaction is properly identified $\geq 75\%$ of the time, even with very low photodiode energy thresholds.

The timing resolution is determined using the method described above, but with a 200 keV energy threshold. The timing distribution, shown in figure 10, has a width of 750 ps fwhm. This width is dominated by the timing jitter of detector module (the timing jitter of the reference detector is expected to be <300 ps), implying that the expected coincidence timing resolution of a pair of these detector modules is 1 ns fwhm, which is a factor of 3 better than is typically achieved with BGO.

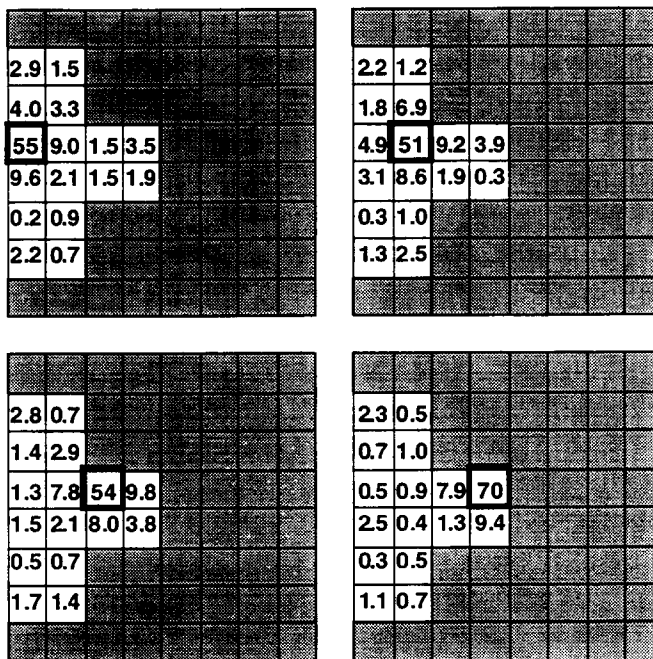


Figure 8: Using the LSO detector, the percentage of the time that each element is identified as the crystal of interaction for four "target" positions (identified by the thick border). Darkened regions indicate elements without amplifiers.

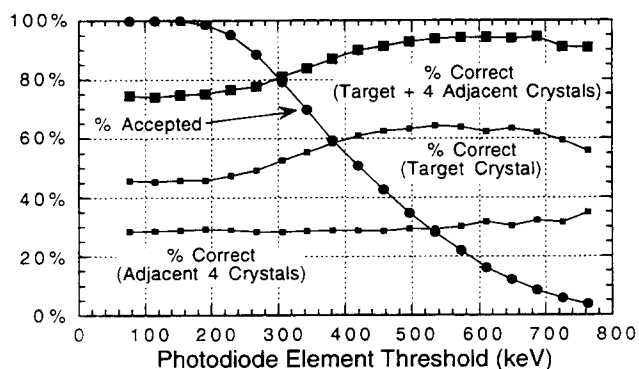


Figure 9: Percentage of events accepted and correctly identified in the LSO detector module as a function of photodiode element threshold voltage. The "target" element used is shown in the upper right portion of figure 8.

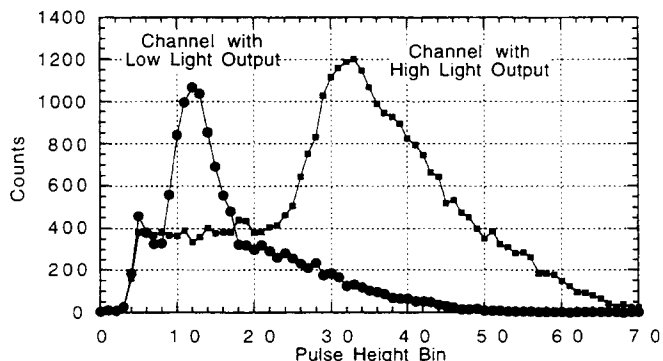


Figure 7: 511 keV pulse height spectra, as observed in the common photomultiplier tube, of two crystals in the LSO module.

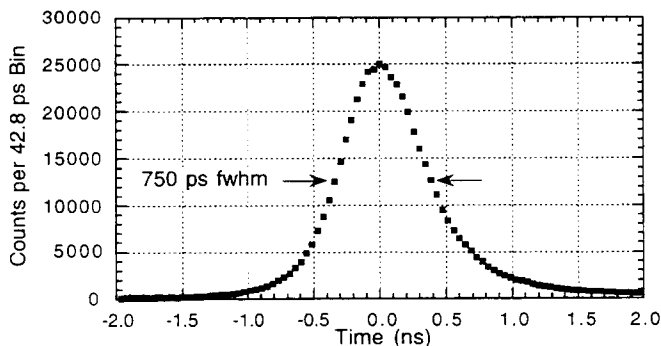


Figure 10: Coincidence timing resolution (with plastic scintillator) for the LSO detector module with a 200 keV threshold.

5. DISCUSSION

The BGO detector module shows moderate performance compared to existing PET detector modules. Its most outstanding feature is its high correct identification fraction, which is typically 65% if only the “target” crystal is considered to be correct and 80% if the adjacent 4 crystals are included as “correct.” The largest drawbacks in its performance are its poor energy and timing resolution, caused by depth of interaction dependence in the crystals. Performance similar to, if not better than, existing block detector modules is expected with a better reflector. However, the lossy reflector may reduce misidentification due to detector Compton scatter, as secondary interactions from Compton scatter tend to occur deep in the crystal, yielding photodiode signals that tend to fall below threshold.

The LSO detector module shows excellent performance compared to existing PET detector modules. The largest drawbacks in its performance (poor energy resolution and channel to channel output variations) can be attributed to the poor quality of the LSO used and the fact that the surface preparation and reflector technology necessary to produce crystals with uniform, high light output is in its infancy. With a more mature technology (*i.e.* the BGO module), channel to channel variations were small enough (even with channels at the edge of the photodiode array) that no such corrections were made, and it is hoped that LSO production and finishing technology can be brought to this level soon. It is also possible that energy resolution will improve if the PD and PMT signals are added together. Finally, higher quality LSO would also allow a practical depth of interaction module to be developed.

While the tendency of these modules to incorrectly place events in the four elements adjacent to the “target” crystal may be considered a drawback, the effect of this misidentification on the spatial resolution is likely to be negligible. With reasonable electronic noise levels, Compton scatter in the detector module produces similar event topologies, and recent simulations indicate that the effect of detector Compton scatter on spatial resolution is minimal [6].

It is also hoped that the next version of the amplifier IC will lead to reliable read out of all 64 channels. This amplifier design (which is presently undergoing testing) should reduce the excess noise due to the design error, provide an additional factor of 5 gain (making the 511 keV output signal well above the WTA threshold), and test a circuit that will allow the gain of each channel to be independently varied (by a factor of 4 in 64 steps) to trim crystal to crystal variations. An array of 4 amplifier ICs and 4 WTA ICs (16 channels each), plus an additional WTA IC to select the highest output of the other 4 WTA “winners” is capable of reading out all 64 channels at a rate of >1 Mhz. In the future, we believe that all of this functionality can be achieved with a 5–6 mm square custom IC.

6. CONCLUSIONS

We have manufactured two 64 element prototype PET detector modules (using BGO and LSO scintillator) in which the crystal of interaction is determined with a photodiode array. With 16 channels instrumented, both detector modules identify

the “proper” crystal of interaction approximately 80% of the time, where the definition of “proper” includes the “target” crystal and the 4 adjacent crystals. With the LSO detector module, the timing and pulse height resolution for 511 keV photons are 750 ps fwhm and approximately 50% fwhm respectively, yielding performance that significantly exceeds conventional BGO based PET detector modules. The BGO detector module has respectable performance, but is limited by poor pulse height and timing resolution. Some improvement may be possible with a different reflector coating or surface treatment. Based on these results, we feel that detector modules based on this design (especially those using LSO scintillator) have tremendous potential in high performance, yet practical, PET cameras.

ACKNOWLEDGMENTS

We would like to thank Mr. Yamamoto of Hamamatsu Photonics for many interesting discussions, culminating with the photodiode array used herein. This work was supported in part by the Director, Office of Energy Research, Office of Health and Environmental Research, Medical Applications and Biophysical Research Division of the U.S. Department of Energy under contract No. DE-AC03-76SF00098, in part by the National Institutes of Health, National Heart, Lung, and Blood Institute, National Cancer Institute, and National Institute of Neurological Disorders and Stroke under grants No. P01-HL25840, No. R01-CA48002, and No. R01-NS29655. Reference to a company or product name does not imply approval or recommendation by the University of California or the U.S. Department of Energy to the exclusion of others that may be suitable.

REFERENCES

- [1] W. W. Moses, S. E. Derenzo, R. Nutt, et al., “Performance of a PET detector module utilizing an array of silicon photodiodes to identify the crystal of interaction,” *IEEE Trans. Nucl. Sci.*, vol. NS-40, pp. 1036–1040, 1993.
- [2] W. W. Moses, S. E. Derenzo, C. L. Melcher, et al., “A room temperature LSO / PIN photodiode PET detector module that measures depth of interaction,” *IEEE Trans. Nucl. Sci.*, vol. NS-42, pp. 1085–1089, 1995.
- [3] W. W. Moses, I. Kipnis, and M. H. Ho, “A 16-channel charge sensitive amplifier IC for a PIN photodiode array based PET detector module,” *IEEE Trans. Nucl. Sci.*, vol. NS-41, pp. 1469–1472, 1994.
- [4] W. W. Moses, E. Beuville, and M. H. Ho, “A “winner-take-all” IC for determining the crystal of interaction in PET detectors,” *IEEE Trans. Nucl. Sci.*, vol. NS-43, (submitted for publication), 1996.
- [5] S. R. Cherry, M. P. Tornai, C. S. Levin, et al., “A comparison of PET detector modules employing rectangular and round photomultiplier tubes,” *IEEE Trans. Nucl. Sci.*, vol. NS-42, pp. 1064–1068, 1995.
- [6] K. A. Comanor and W. W. Moses, “Algorithms to identify detector Compton scatter in PET modules,” *IEEE Trans. Nucl. Sci.*, vol. NS-43, (submitted for publication), 1996.